Photo-induced and thermal reactions in thin films of an azobenzene derivative on Bi(111)

2014 New J. Phys. 16 053004

(http://iopscience.iop.org/1367-2630/16/5/053004)

New Journal of Physics
The open access journal at the forefront of physics
Deutsche Physikalische Gesellschaft DPG | IOP Institute of Physics

Photo-induced and thermal reactions in thin films of an azobenzene derivative on Bi(111)

Christopher Bronner[1,2] **and Petra Tegeder**[1]

[1] Ruprecht-Karls-Universität Heidelberg, Physikalisch-Chemisches Institut, Im Neuenheimer Feld 253, D-69120 Heidelberg, Germany
[2] Freie Universität Berlin, Fachbereich Physik, Arnimallee 14, D-14195 Berlin, Germany
E-mail: bronner@uni-heidelberg.de

Received 7 January 2014, revised 13 March 2014
Accepted for publication 24 March 2014
Published 1 May 2014

New Journal of Physics **16** (2014) 053004

doi:10.1088/1367-2630/16/5/053004

Abstract

Azobenzene is a prototypical molecular switch which can be interconverted with UV and visible light between a *trans* and a *cis* isomer in solution. While the ability to control their conformation with light is lost for many molecular photoswitches in the adsorbed state, there are some examples for successful photoisomerization in direct contact with a surface. However, there the process is often driven by a different mechanism than in solution. For instance, photoisomerization of a cyano-substituted azobenzene directly adsorbed on Bi(111) occurs via electronic excitations in the substrate and subsequent charge transfer. In the present study we observe two substrate-mediated *trans–cis* photoisomerization reactions of the same azobenzene derivative in two different environments within a multilayer thin film on Bi(111). Both processes are associated with photoisomerization and one is around two orders of magnitude more efficient than the other. Furthermore, the *cis* isomers perform a thermally induced reaction which may be ascribed to a back-isomerization in the electronic ground state or to a phenyl ring rotation of the *cis* isomer.

Keywords: molecular switches, two-photon photoemission, photoisomerization, Bi(111), azobenzene

1. Introduction

Molecular switches are a class of molecules which are bistable and can be inter-converted from one form to the other by manipulating them using light, electrons, heat or other external stimuli. The two forms may differ in their geometrical structure, spin configuration, dipole moment or other properties. They are of considerable interest to both technological applications and fundamental research. Molecular switches can for example be used to introduce functionality to larger molecular units and thus allow control over their properties [1]. Incorporated into self-assembled monolayers, molecular switches can be used to make functionalized surfaces, the macroscopic properties of which can be altered by changing the state of the switches [2–4]. Furthermore, many molecular switches are organic compounds and physisorb on metallic surfaces which makes them interesting to benchmark developments in density functional theory that include corrections to account for dispersive van der Waals-interactions [5–7].

Since light is a relatively non-invasive and experimentally convenient way of manipulating such systems, a particular focus lies on photochromic molecular switches. Among them, azobenzene is especially prominent due to its relatively simple structure. In solution, azobenzene can be transformed from its *trans* to its *cis* isomer with UV light and this photoisomerization is reversible with visible light or thermally [8]. In the light-driven reactions, the ground state barrier between the two isomers is overcome by relaxation of the photo-excited molecule on the potential energy surface of a higher-lying electronic state [9, 10]. The isomerization ability of molecular switches is often quenched when the molecule is adsorbed directly on a metal surface [11–16]. This loss of functionality is frequently ascribed to the emergence of efficient de-excitation pathways due to electronic coupling to the metal, or to a strong interaction between the highly polarizable electronic system of the phenyl rings and the substrate due to van der Waals forces. On the other hand, there are also examples of adsorbed photoswitches with intact (or restored) isomerization capability in direct contact with a metal, semi-metal or semiconductor surface [17–20].

While these studies deal with molecules adsorbed in the first monolayer, other experiments have also demonstrated the conservation of photoisomerization ability of molecular switches in the multilayer (i.e. in the second or higher layers of an adsorbate film). In fact, decoupling of the photochromic unit from the substrate allows photo-switching for a broad range of molecular switches based on spiropyran [21], azobenzene [14], imine [22] and diarylethene [23]. Derivatives of azobenzene have even been shown to remain interconvertible in a condensed bulk phase, despite the large geometrical change during isomerization: exposure of a single crystal of the *trans* isomer with UV light leads to a macroscopic bending of the entire solid which can be reversed thermally [24]. Similarly, a macroscopic molecular crystal based on diarylethene contracts upon irradiation with UV light and this process is reversible using visible light [25].

In this study we use a cyano-substituted azobenzene derivative, di-meta-cyano-azobenzene (DMC, see figure 1). The electronegative cyano groups are thought to withdraw electron density from the bonding π-type orbitals of the photochromic diazo bridge (–N=N–) in the center of the molecule. A weakened –N=N– double bond reduces the barrier for rotation around this bond, which should allow for more efficient interconversion since rotation is one of the two pathways (the other one being inversion) for isomerization [26]. In a scanning tunneling microscope (STM) junction, the tunneling electrons cause different reactions of DMC adsorbed on metal surfaces: on the Cu(100) surface, *trans*-DMC can be irreversibly converted to the *cis* form

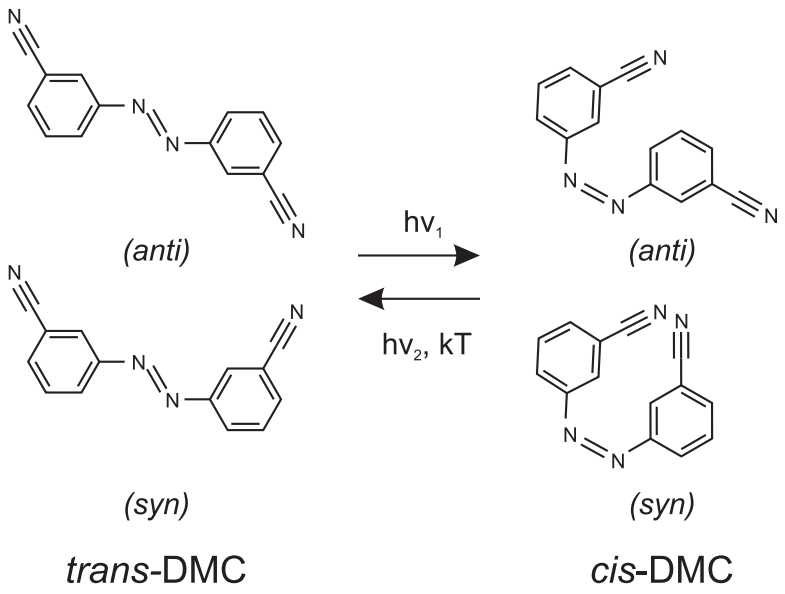

Figure 1. *Trans* and *cis* isomers of DMC and the reaction pathways between them in solution. Both isomers occur in two different rotamers which differ in the relative position of the cyano groups and are labeled *syn* and *anti*, respectively.

which is stabilized by a partially covalent character of the N–Cu bond in the *cis* state [27]. On the Au(111) surface, the tunneling electrons of the STM stimulate a rotation of one of the phenyl rings around the C–N bond, but isomerization has not been observed, most likely due to the strong van der Waals interaction of the aromatic π system of the phenyl rings with the gold substrate or efficient quenching of excited states [12]. Together with cobalt adatoms, DMC forms metal-organic networks on Au(111) [28].

We have previously observed a photo-induced *trans–cis* reaction in the first layer of DMC on the semi-metallic Bi(111) surface. This photoisomerization can be induced over a broad spectral range in the UV regime by excitation of electrons in the substrate *p*-bands. Following this excitation, hot electrons tunnel into the lowest unoccupied molecular orbital (LUMO) of DMC, creating a negative ion resonance which eventually drives the conformational change toward the *cis* isomer [29].

In the present contribution we find that DMC undergoes two different photo-induced *trans–cis* isomerization reactions in two different environments of the multilayer regime of DMC on Bi(111), one of which has a similar cross section as the photoisomerization in the first monolayer while the cross section of the other process is approximately two orders of magnitude higher. Both reactions are assigned to a photo-induced *trans–cis* isomerization. Furthermore, the *cis*-DMC isomers undergo a thermally activated reaction which may be due to a *cis–trans* back-isomerization or a phenyl ring rotation of *cis*-DMC.

2. Experimental methods

A Bi(111) single crystal was mounted in ultra-high vacuum (UHV) on a flow cryostat equipped with resistive heating facilities which was operated with either liquid nitrogen (LN_2) or liquid helium (LHe) (in the Auger electron spectroscopy (AES) experiments which were carried out in

Table 1. AES peak positions for various elements in our experiments and in the literature.

In (eV)	Bi	Bi	Bi	Bi	C	N	O
Experiment	110	137	264	283	283	399	—
Literature [35]	101	129	249	268	272	381	510

another UHV chamber, a bath cryostat was used with LN_2 only). This allowed for precise control of the sample temperature from around 70 K (using LHe) up to the annealing temperature of Bi (410 K). For most measurements, the sample was cooled to around 100 K using LN_2, LHe was used only in the experiments on the thermally induced reaction. The Bi(111) substrate was prepared by Ar^+ sputtering (ion energy of 1 keV) and subsequent annealing at 410 K (400 K in AES experiments) for 10 min. DMC was evaporated from a Knudsen cell at a temperature of 107 °C (120 °C in AES experiments) onto the substrate which was held at 120 K (150 K in AES experiments).

The photo-induced reaction of multilayer DMC is characterized by changes in the work function, as observed in photoemission spectra recorded with a time-of-flight spectrometer. Due to the wide range of photon energies employed, photoemission signals vary in their nature: for photon energies $h\nu$ higher than the work function of the sample Φ, directly photo-emitted electrons are observed. When $\Phi > h\nu > \Phi/2$, the signal is dominated by two-photon photoemission [30–32] and when $h\nu < \Phi/2$, three-photon photoemission is the predominant process. We display all spectra versus the final state energy E_{Final} of the photo-emitted electron, referenced to the Fermi level E_{F}, which is essentially the kinetic energy of the photoelectron E_{kin} plus the work function, $E_{\mathrm{Final}} - E_{\mathrm{F}} = E_{\mathrm{kin}} + \Phi$.

A Ti:Sapphire oscillator provided femtosecond laser pulses which were amplified in a regenerative amplifier and subsequently converted into the visible spectrum using an optical parametric amplifier and frequency-doubled into the UV regime using a BBO crystal. The laser setup is described in detail elsewhere [15, 17, 33, 34]. In the illumination experiments, the photon flux and energy fluence varied from measurement to measurement but were always on the order of $10^{19\pm1}\,\mathrm{cm^{-2}s^{-1}}$ (photon flux) and $10^{-2\pm1}\,\mathrm{mJ\,cm^{-2}}$ (energy fluence), respectively.

AES experiments were conducted in a different UHV chamber which was equipped with similar facilities for sample preparation and characterization and additionally a cylindrical mirror analyzer (Omicron CMA150) with an integrated electron gun. Note, that the analyzer was not efficiently calibrated, thus the measured electron energies are approximately 10 eV too high (see table 1).

3. Results

We observed reactions induced by light and thermal activation in the multilayer of DMC, which are described in this section as follows. First, we discuss experiments characterizing the adsorbate, then, using photoemission we demonstrate two photo-induced isomerization processes (section 3.2). Finally, in section 3.3, we report on a thermally induced process for *cis* isomers of DMC in the multilayer and in the first monolayer, respectively.

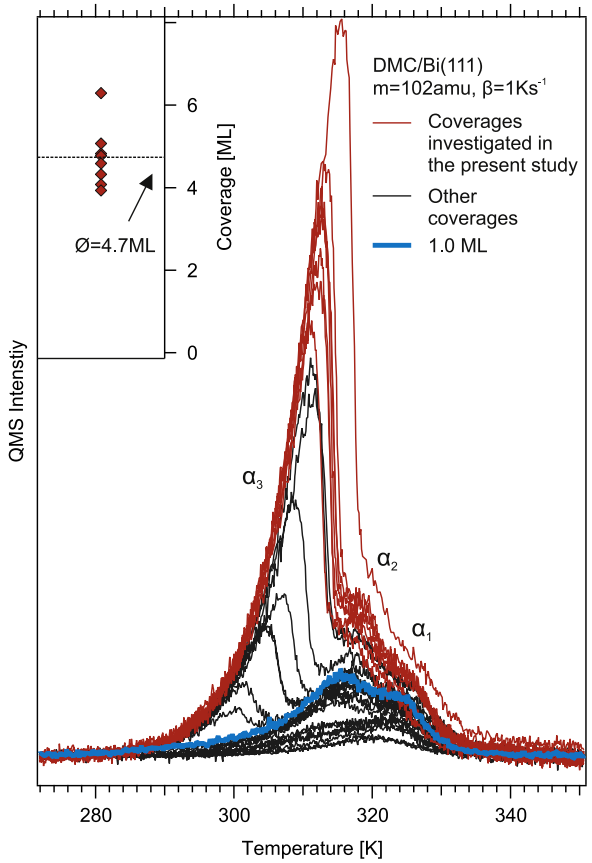

Figure 2. TPD curves for varying initial coverages of DMC, exhibiting two desorption features (α_1, α_2) assigned to the first monolayer and one (α_3) arising from multilayer desorption. The thick, blue line indicates the TPD of one monolayer and the red lines indicate those preparations which were used in the measurements presented in this contribution. For those, the inset shows the coverages determined by integration of the TPDs.

3.1. Sample characterization

In order to characterize the adsorbate coverage, we employed temperature programmed desorption (TPD) where fragments of the desorbing molecules are detected using a quadrupole mass spectrometer. For detection of DMC, we followed the fragment mass of 102 amu, corresponding to a phenyl ring substituted with a cyano group ($C_6H_4\,CN^+$). Figure 2 shows a series of TPD curves for different initial coverages of DMC. We observe three desorption features, two of which saturate with increasing initial coverage (α_1 and α_2) while a third feature α_3 rises indefinitely with a peak shape typical for zero-order desorption from the multilayer. For a detailed discussion see [29]. The initial coverage was varied via the evaporation time and measured by integration of the TPD curves after subtraction of a linear background. The integral was normalized to the peak area of the TPD of a full monolayer (blue curve in figure 2). The TPD curves shown in red in figure 2 represent the preparations which were used for the experiments shown in this study, where the average coverage was 4.7 ML (see inset in figure 2).

Following the behavior of substrate and adsorbate peaks, respectively, in AES with increasing adsorbate coverage allows to discriminate between three growth modes. In case of Volmer–Weber growth (islands), the substrate peak (Bi) should decrease in intensity with rising DMC coverage, but should never be fully quenched. The same is true for Stransky–Krastanov growth (wetting layer and islands on top) because the single wetting layer does not completely quench the substrate signal in those areas where no islands are growing. Only for Frank–van der Merwe (layer-by-layer) growth does the substrate peak vanish completely [36].

We first prepared a clean Bi(111) substrate, then we recorded an AE spectrum, evaporated a certain amount of DMC and recorded another AE spectrum under the same conditions. Both AE spectra of such a preparation cycle were normalized using the same factor such that all AE spectra of bare Bi(111) would have the same substrate peak intensities. We repeated this procedure several times for various DMC coverages and the results are shown in figure 3(a).

The spectrum of the clean substrate shows one intense feature at 110 eV and three less pronounced ones, in agreement with literature (see table 1). With increasing DMC coverage, the substrate features are quenched and two new features arising from C (283 eV) and N (399 eV) continuously gain intensity. The intensities of the substrate and adsorbate peaks, respectively, are shown as a function of DMC coverage in figure 3(b). The dominant feature of the substrate at 110 eV is quenched exponentially with increasing coverage. Fitting the coverage-dependent Bi peak intensity, we find an attenuation length of 2.3 ± 0.4 ML. The intensities of the N and C features, respectively, rise in the same fashion with an N:C intensity ratio of 0.26 ± 0.03. Considering that from the structure of the DMC molecule, a N:C ratio of 4:14 = 0.29 would be expected, this demonstrates that the adsorbate is clean. The complete quenching of the substrate peaks, which we observe at coverages exceeding 10 ML, is indicative of Frank–van der Merwe (layer-by-layer) growth.

While conducting the AES experiments, we noticed changes in the adsorbate film which were induced by the high-energy electrons. Upon exposure to the electron beam, the molecules in the multilayer could not be desorbed at 400 K, in contrast to the results shown above. After recording a TPD, the C and N features associated with the adsorbate in the AE spectra could still be observed, possibly due to an electron-induced polymerization reaction.

3.2. Light-induced reaction observed with photoemission

In order to elucidate photo-induced reactions in the DMC film, we evaluated the changes in the work function upon light exposure. Figure 4(a) shows a series of direct photoemission spectra during an illumination experiment. With increasing photon dose, the work function increases by around 500 meV. Qualitatively, this behavior is the same as the work function increase during photoisomerization of *trans*-DMC in the first monolayer [29]. However, the changes in the multilayer occur at much lower photon doses, which indicates a more efficient process. The work function increase as a function of photon dose is shown in figure 4(b). The data do not follow a simple exponential behavior. Instead, they can be fitted with a bi-exponential function,

$$\Phi(d) = \Phi(0) + \frac{\Delta\Phi}{\gamma} \times \left[1 - e^{-\sigma_1 d} - \gamma e^{-\sigma_2 d}\right]. \quad (1)$$

Here, $\Delta\Phi$ is the asymptotic work function change, $\sigma_{1,2}$ are two different effective cross sections and γ describes the ratio of the two components' influence on the work function change. All these parameters are varied in the fits. For the data shown in figure 4(b), the two

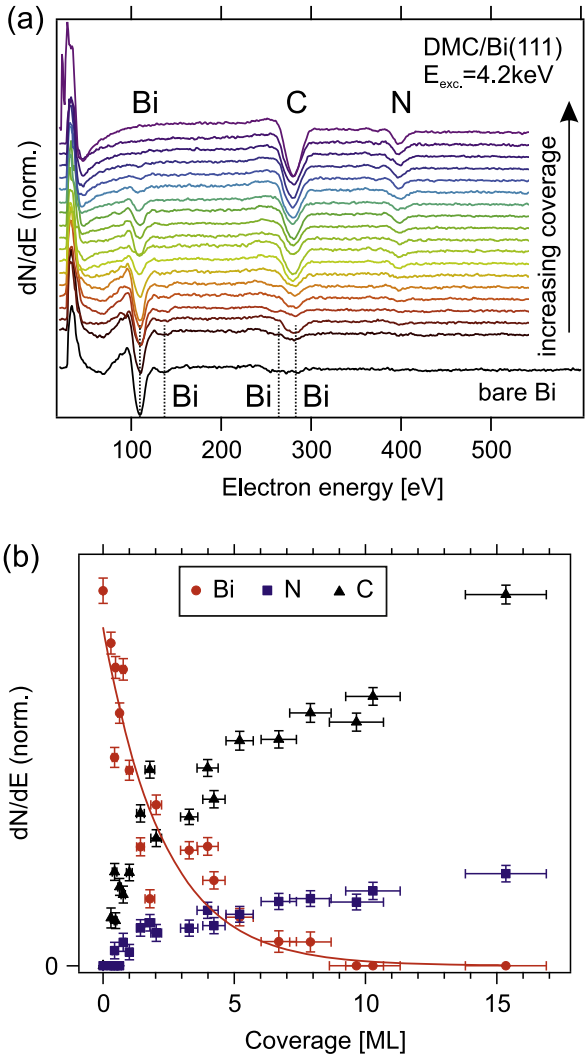

Figure 3. (a) AE spectra for the bare Bi(111) substrate and increasing DMC coverages. The spectra were normalized by the signal of the Bi peak at 110 eV (see text). (b) Change in peak intensity of the Bi, N and C peaks at 110 eV, 399 eV and 283 eV, respectively. The same data set as in (a) is shown. The quenching of the Bi feature has been fitted with an exponential function (solid line).

cross sections amount to $\sigma_1 = 4.0 \pm 0.4 \times 10^{-21}$ cm^2 and $\sigma_2 = 3.4 \pm 0.3 \times 10^{-23}$ cm^2. Hence, there are two different reactions, one being two orders of magnitude more effective than the other. A qualitatively similar behavior is observed over a wide range of photon energies. Besides an energetic shift of the secondary edge (the low-energy cutoff), one can also observe a change of its width: first, the width increases, then, as the work function reaches 4.2 eV, it narrows again and then rises once again. This behavior can be understood as a broadening of the work function during each of the two reactions. The broadening is owed to the spatially inhomogeneous laser spot which has a higher intensity in the center and therefore, a light-induced reaction occurs faster there than in the outer regions [37]. When the reaction has saturated in the center of the spot, the more slowly changing work function in the outer regions

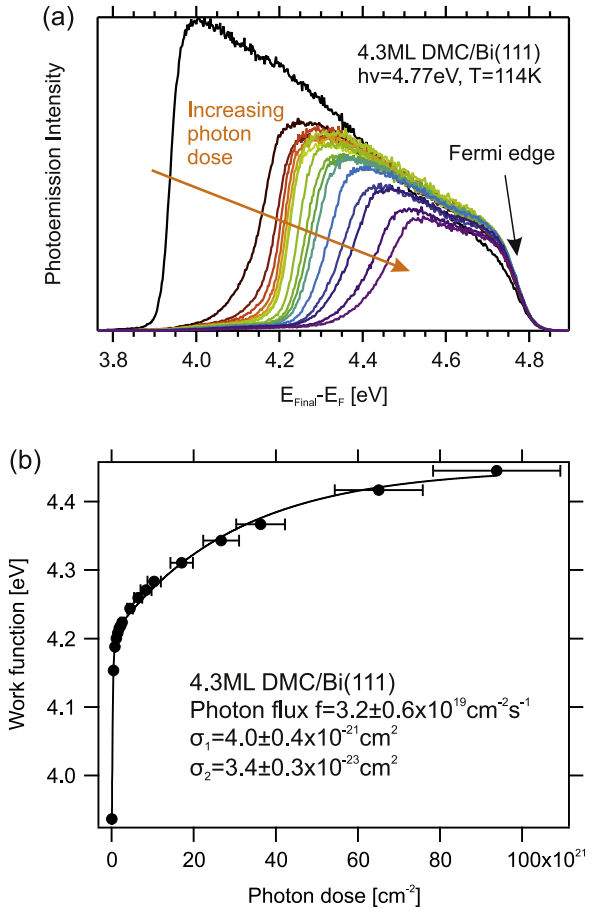

Figure 4. (a) Light-induced changes in the photoemission spectra with increasing photon dose. (b) Evolution of the work function during illumination. The solid line represents a bi-exponential fit to the data.

can 'catch up' and the secondary edge is reduced in width again. The same then happens again for the second reaction on a longer timescale.

Both photo-induced processes can be observed over a wide range of photon energies in the UV regime, as shown in figure 5. Over the entire range, the effective cross section of the more efficient process is approximately two orders of magnitude larger than the one for the other reaction and the cross section of the less efficient process is relatively close to the cross section observed for the photoisomerization in the first monolayer.

For both reactions, the cross section increases exponentially with increasing photon energy. This behavior is qualitatively the same for the photoisomerization reaction in the first monolayer which has been identified as a substrate-mediated process because the broad range of excitation energies contradicts a resonant intramolecular excitation mechanism [29]. The same argument holds for the multilayer reactions and surprisingly, we do not observe any increase in the cross section at the energies of the $\pi\pi^*$- or $n\pi^*$-transition of the free molecule or at the energy of the HOMO–LUMO gap of DMC in the first monolayer. Thus, we exclude direct electronic transitions within the molecule to be the main excitation pathway for the reaction. The exponential cross section increase observed for both reactions in the multilayer furthermore

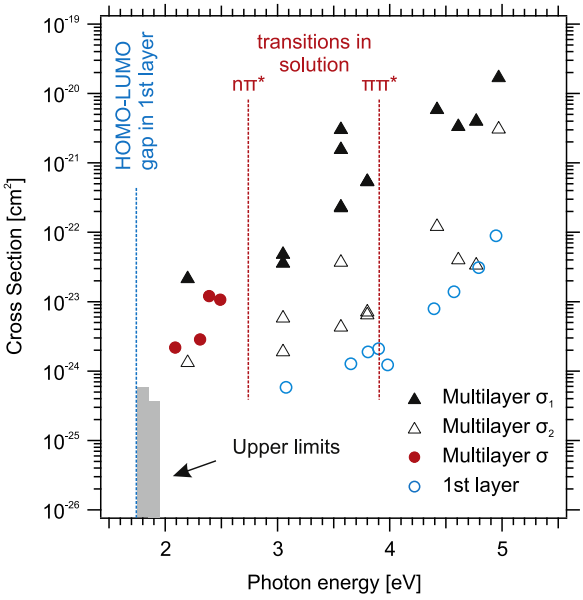

Figure 5. Photon energy dependence of the effective cross sections. The values measured in the multilayer (full triangles, open triangles, full red circles) are compared to the cross sections in the first monolayer (open blue circles) [29]. For photon energies below 2 eV, the upper limits for the cross section are stated and the dashed lines indicate relevant electronic transitions in the first layer and for DMC in solution.

is a counter-indication for a thermally induced reaction for which the cross section would be proportional to the photon energy and thus would depend linearly on the photon energy. On the other hand, the observed strong increase of the cross section with increasing photon energy is characteristic for adsorbate reactions that are induced by hot electron transfer from the substrate [38, 39].

While spectral changes are observed for a broad range of excitation energies, no such changes are found in the photon energy regime below 2 eV. However, due to limitations in the photon dose which the sample can be exposed to, there is of course a detection limit for very inefficient reactions with a low cross section. Based on the applied photon dose we can determine upper cross section limits for photon energies below 2 eV, which are indicated in figure 5. For most other photon energies, two cross section components are necessary to describe the spectral changes similarly to figure 4(b). In contrast, between 2.0 eV and 2.5 eV, the photo-induced work function increase can be well fitted with a mono-exponential function, except for one photon energy (red full circles in figure 5). This may be due to the lower cross section component falling below the detection limit in this region.

In summary, we observe two substrate-mediated, non-thermal processes in the multilayer which are induced by light of various wavelengths. The photon energy dependent behavior of the effective cross sections is identical to the one found for the photoisomerization in the first monolayer [29] and for one of the reactions, the efficiency is on the same order of magnitude as in the first layer. Therefore, and based on the results of the thermally induced reaction (section 3.3) we assign these reactions to *trans–cis* photoisomerization processes which are common for molecular switches in multilayers on metal substrates [14, 21–23].

The difference between the effective cross section of the two isomerization reactions is most likely due to the location of the involved molecules within the film: there are essentially three different molecular environments and we can use them to discriminate the DMC molecules in our system, namely those in the first monolayer, those in the 'bulk' multilayer and those in the topmost layer at the vacuum interface. While steric hindrance should be important, particularly for the first two cases, one should note that an azobenzene derivative has been observed to even perform a photo-induced *trans–cis* reaction in the bulk [24], despite a considerable change of the molecular geometry. We can therefore not rule out any reactions in the multilayer or at the substrate–adsorbate interface.

The efficiencies (i.e. the cross sections) of the two isomerization processes are influenced by a number of aspects. As mentioned above, steric hindrance would be expected to be much lower at the adsorbate–vacuum interface, possibly increasing the efficiency there. However, the tunneling barrier for the charge carriers which tunnel from the substrate into the electronic states of the adsorbate is drastically increased with rising distance of the molecular unit from the substrate. For molecules at the adsorbate–vacuum interface, these two effects are competing and therefore one can not say whether the efficiency, as represented by the cross section, of photoisomerization induced by charge carriers tunneling from the substrate into the adsorbate is more or less efficient at one of the three possible positions within the film.

3.3. Thermal reaction of the cis*-isomers*

Using photoemission, we can observe another kind of reaction in the multilayer regime of DMC on Bi(111). When the photo-produced phase (henceforth labeled B) of the light-induced reaction $\left(\mathrm{A} \rightarrow \mathrm{B}\right)$ described in section 3.2 is annealed, the work function decreases. From now on the state after the annealing step will be labeled C. For the following, DMC was evaporated onto the clean substrate and subsequently annealed to 240 K for 30 min so that the temperature-induced changes described below can unambiguously be assigned to the *cis* isomers within phase B. Figure 6(a) shows the following three-step experiment repeated with different annealing temperatures and always on a new spot: (i) the first spectrum (black) is recorded on the all-*trans* sample, as it was prepared. (ii) The DMC film (state A) was then illuminated with a dose of $d = 2.6 \times 10^{21}\,\mathrm{cm}^{-2}$ using the same laser beam which was used for the photoemission experiments shown here ($h\nu = 4.93$ eV). Then, a second photoemission spectrum was recorded (blue). Note that in this state (B), the photoisomerization processes have not saturated (this would not be practically feasible due to the low cross section). Especially the inefficient reaction has had little effect on the system in this state yet. Although the processes have not saturated, in all experiments shown here, the state after illumination (B) is equivalent due to the constant photon dose applied. This is important because in order to employ an Arrhenius type evaluation, the initial state of the thermal reaction (B) must be equivalent for every annealing experiment. This equivalence of the illuminated state was furthermore verified by the photoemission spectra recorded afterwards (blue) which show no differences between the single annealing experiments. (iii) In the third step, the sample was heated to a specific temperature in the range of 80 K to 240 K for 5 min and subsequently, another photoemission spectrum was recorded in the resulting state C (red).

With increasing annealing temperature, the work function is more and more reduced after the heating step and we use this work function change to quantify the temperature-induced

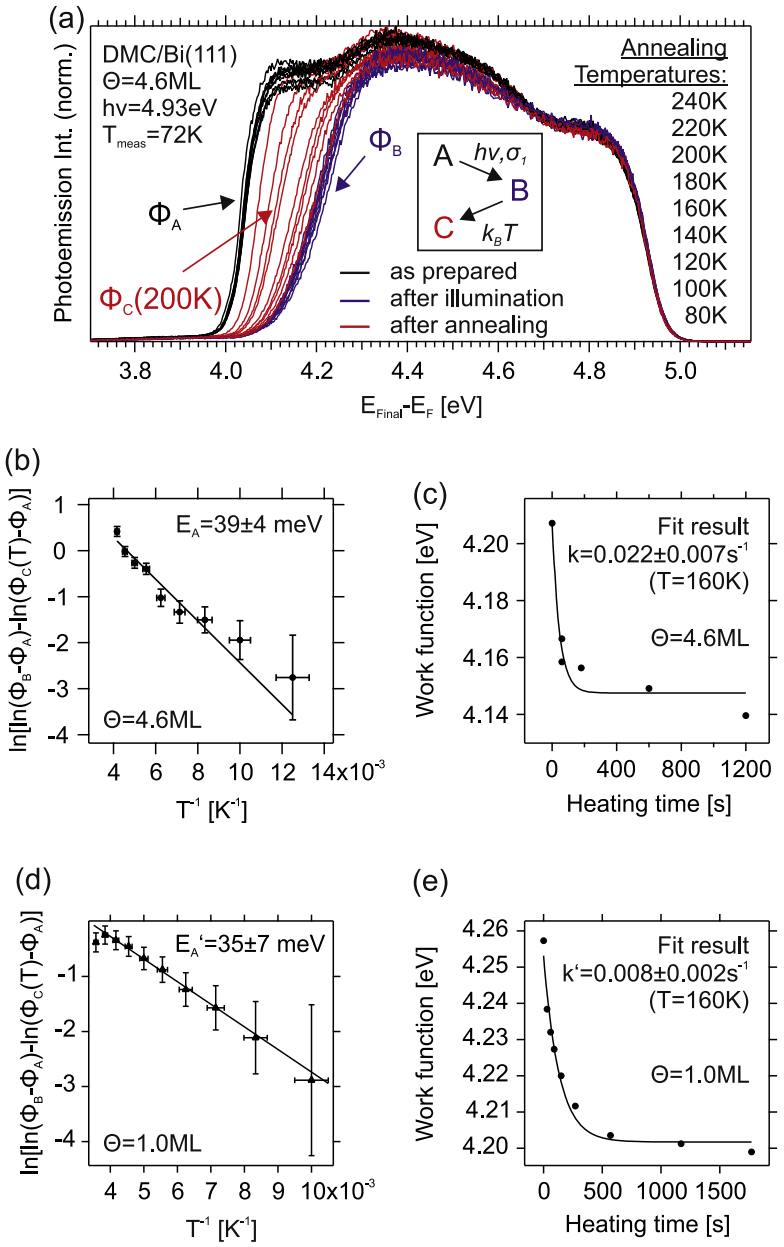

Figure 6. (a) Photoemission spectra of multilayer DMC after deposition (black), after illumination (blue) and after subsequent heating to a specific temperature (red, 5 min). All spectra were recorded at a sample temperature of 72 K. The inset schematically shows the involved reactions of DMC. (b) Arrhenius plot for the thermal reaction in the multilayer, resulting from the series shown in (a). A measure for the changes of the work function (see text for details) is plotted over the inverse annealing temperature. (c) Work function change as a function of annealing time at 160 K. A fit according to equation (2) yields the rate constant at this temperature. (d) Arrhenius plot analogous to (b) but for a DMC coverage of 1.0 ML. (e) Determination of the rate constant at 160 K for a coverage of 1.0 ML, in analogy to (c).

reaction. In a first order thermal reaction B → C, the concentration of molecules in state B is

$$[\mathrm{B}] = [\mathrm{B}]_0 \exp(-kt), \tag{2}$$

with $[\mathrm{B}]_0$ the initial concentration. The temperature dependence of the rate constant k is described by an Arrhenius-type expression,

$$k(T) = k_0 \exp\left(-\frac{E_\mathrm{A}}{k_\mathrm{B}T}\right). \tag{3}$$

Here, k_0 is the pre-exponential factor and E_A denotes the activation energy. Using the work function $\Phi_\mathrm{C}(T)$ in state C, which depends on the annealing temperature T, as a measure for the change of the number of *cis* molecules, $[\mathrm{B}] \propto \Phi_\mathrm{C}(T) - \Phi_\mathrm{A}$, we obtain the following expression for the temperature-dependence of $\Phi_\mathrm{C}(T)$:

$$\ln\left[\ln\left(\Phi_\mathrm{B} - \Phi_\mathrm{A}\right) - \ln\left(\Phi_\mathrm{C}(T) - \Phi_\mathrm{A}\right)\right] = -\frac{E_\mathrm{A}}{k_\mathrm{B}T} + \text{ const.} \tag{4}$$

The work function values after the annealing step, $\Phi_\mathrm{C}(T)$, are shown in the form of equation (4) over the inverse temperature in figure 6(b), yielding an activation energy for the thermally induced process of $E_\mathrm{A} = 39 \pm 4$ meV. This value will be discussed below with respect to its relatively low magnitude.

In order to determine the pre-exponential factor (the attempt frequency) of the temperature-induced reaction B → C, we conducted an additional, slightly different annealing experiment. The sample was prepared as described above and illuminated with the same photon dose, resulting in state B. Then, we annealed the sample at a temperature of 160 K for a defined heating time t and recorded a photoemission spectrum. This was repeated several times and figure 6(c) shows the evolution of the work function during heating. Note, that we cooled the sample to a temperature of 72 K while recording the spectra. Assuming again a proportionality between the concentration of *cis* molecules in state B and the work function change, we fitted the work function change with an expression derived from equation (2) and obtain the temperature-specific rate constant $k(T = 160\ \mathrm{K}) = 0.022 \pm 0.007\ \mathrm{s}^{-1}$. Using equation (3) we therefore find a pre-exponential factor of $k_0 = 0.37 \pm 0.16\ \mathrm{s}^{-1}$ which will be discussed after a comparative experiment in the first monolayer.

We conducted the same kind of annealing experiments, which were described above, for a coverage of 1.0 ML in order to compare the results for the two coverage regimes. The sample was prepared as in the multilayer, except that a monolayer was produced by heating the sample to 300 K for approximately 1 min directly after deposition, which leads to a desorption of the second and higher layers [29].

Figure 6(d) shows the Arrhenius graph for the first monolayer from which we obtain an activation barrier of $E'_\mathrm{A} = 35 \pm 7$ meV. The data point at highest annealing temperature (280 K) does not follow the expected behavior which is due to partial desorption (see figure 2). We can fit the time-dependent work function change in analogy to the experiment in the multilayer, resulting in a rate constant at 160 K of $k'(T = 160\ \mathrm{K}) = 0.008 \pm 0.002\ \mathrm{s}^{-1}$ and a pre-exponential factor of $k'_0 = 0.10 \pm 0.06\ \mathrm{s}^{-1}$. The activation energy is identical to the one in the multilayer whereas the pre-exponential factor is lower in the first monolayer but on the same

order of magnitude. Another interesting result of the annealing experiments in the first layer is that by thermal activation, the original spectrum (before illumination) can not be restored, even for long heating times. This behavior is not consistent with only a thermally induced *cis–trans* reaction.

Comparing the results of the annealing experiments in the first monolayer and in the multilayer, one striking observation is that the results are so similar. Due to heating of the monolayer and the multilayer films at 240 K for 30 min before the respective illumination and annealing experiments we can be certain that the thermal reaction observed here occurs only for those molecules which have previously reacted under the influence of the light. Since the activation energy is identical and the pre-exponential factor is on the same order of magnitude for both coverage regimes, we conclude that the observed thermal reaction is the same. Therefore, if the very same process occurs for the two photo-products of the two coverage regimes, it is very likely that the photo-products themselves are identical, which supports our interpretation that the light-induced processes observed in the multilayer are due to *trans–cis* photoisomerization.

Having discussed the implications of the thermally induced reaction for the photoisomerization of DMC, the question about the nature of the observed reaction remains. In the comparable system TBA (tetra-*tert*-butyl-azobenzene)/Au(111), a thermally activated *cis–trans* reaction is observed after a *trans–cis* photoisomerization. The activation barrier for this reaction was reported to be 240 ± 30 meV [40]. In the same study, the activation barrier for thermal *cis–trans* isomerization of TBA in solution was measured and amounts to 1.01 ± 0.03 eV. In a theoretical study, this value for isolated TBA is calculated to 1.39 eV and the corresponding barrier for isolated DMC is 1.03 eV [26]. Besides azobenzenes, other molecular switches also perform thermal isomerization reactions at surfaces. For a spiropyran derivative, a thermally induced ring-opening reaction with an activation barrier of 840 ± 50 meV is observed [41] and the thermal isomerization reaction of an imine derivative has an activation energy of 0.6 ± 0.1 eV [42]. For DMC on Bi(111) we find that the activation barrier in both coverage regimes is 37 meV (averaged). Compared to the values for molecular isomerization reactions found in literature, this value seems rather small. Furthermore, as already mentioned we do not observe a complete restoration of the original spectra upon heating in the monolayer, which speaks against back-isomerization reaction.

As seen in figure 1, each DMC isomer has two different rotamers, depending on the relative position of the cyano groups. An alternative explanation for the observed thermal process could therefore be a rotation of one of the phenyl rings, changing the position of the cyano group from *syn* to *anti* in the *cis*-DMC isomer. As the rotamers are equally distributed in the *trans* form, this reaction can thus only occur for half of the *cis* molecules. Since the rotation is around a σ bond, the barrier would arise mainly due to the transient repulsion of the two rings and should be significantly smaller than the barrier for an isomerization which involves a transient breaking of the double bond at the diazo bridge. Since at least one cyano-substituted phenyl ring in the *cis* isomer can be expected to be tilted with respect to the surface plane, the steric barrier for rotation posed by the substrate or underlying layers should have less influence than it would have in the *trans* isomer. In the literature, the rotational barrier of a phenyl ring group in a comparable molecule is calculated to be 37 meV in the gas phase which corresponds remarkably well to the barrier that is observed in the present study [43]. However, one has to

keep in mind that in our case, the molecule is adsorbed on a surface, even if the interaction with the surface is reduced in the *cis* geometry.

The fact that the work function change in the *trans–cis* isomerization is an increase rather than a decrease, indicates a geometry of the *cis* molecule in which the cyano groups are generally pointing toward the vacuum. Therefore, a thermally induced *syn–anti* reaction would be consistent with a rotation which brings one electro-negative cyano group closer to the surface and into an in-plane orientation.

The observed pre-exponential factor (or attempt frequency) in both coverage regimes is on the order of 0.1 Hz which is very low for a pre-exponential factor in general and particularly compared with the one found for the thermally induced *cis–trans* reaction of TBA/Au(111), which amounts to $10^{6\pm1}$ s^{-1} [40]. The pre-exponential factor for TBA in solution is even larger, namely 1.6×10^{10} s^{-1}. Considering the above proposed *syn–anti* rotation as the thermally induced process, it is conceivable that the potential energy surface is rather flat along the rotational coordinate corresponding to a phenyl ring rotation because it is a rotation around a σ bond. Due to the shallow potential minimum, the vibrational frequency of the mode associated with a rotation of the phenyl ring can expected to be rather low which could result in a small pre-exponential factor. In a comparable system which performs a phenyl ring rotation on a surface [43], the pre-exponential factor amounts to 10^{6} s^{-1}. However, there the phenyl rings are adsorbed in a flat geometry and the interaction with the surface can be expected to considerably change the potential for rotation around the σ bond, compared to the twisted geometry of the *cis*-DMC isomer in the present study.

4. Conclusion

Using different external stimuli we could induce various reactions of DMC within a multilayer adsorbed on the Bi(111) surface. In photoemission experiments, we observe two different substrate-mediated *trans–cis* photoisomerization reactions involving DMC in two different environments which are induced by light ranging from the visible to the UV regime. One of the processes is two orders of magnitude more efficient than the other. Both in a monolayer and in the multilayer regime, a thermally induced reaction of the *cis*-DMC isomers is observed which has an activation barrier of 37 meV and might be due to a *cis–trans* reaction in the electronic ground state or a rotation of one of the phenyl rings, changing the molecular conformation of the *cis* isomer from *syn* to *anti*.

Acknowledgments

We would like to thank Judith Specht who assisted in the monolayer annealing experiments in the framework of her BSc thesis at the Freie Universität Berlin. We would furthermore like to acknowledge Beate Priewisch and Karola Rück-Braun (Technische Universität Berlin) for providing the DMC molecules. Stimulating discussions with Reinhard Maurer (Technische Universität München) are much appreciated. Funding by the German Research Foundation (DFG) through Collaborative Research Center SFB658 is gratefully acknowledged.

References

[1] Venkataramani S, Jana U, Dommaschk M, Sönnichsen F D, Tuczek F and Herges R 2011 Magnetic bistability of molecules in homogeneous solution at room temperature *Science* **331** 445–8

[2] Ichimura K, Oh S-K and Nakagawa M 2000 Light-driven motion of liquids on a photoresponsive surface *Science* **288** 1624–6

[3] Liu D, Xie Y, Shao H and Jiang X 2009 Using azobenzene-embedded self-assembled monolayers to photochemically control cell adhesion reversibly *Angew. Chem. Int. Ed.* **48** 4406–8

[4] Klajn R 2010 Immobilized azobenzenes for the construction of photoresponsive materials *Pure Appl. Chem.* **82** 2247–79

[5] Mercurio G *et al* 2010 Structure and energetics of azobenzene on Ag(111): benchmarking semiempirical dispersion correction approaches. *Phys. Rev. Lett.* **104** 036102

[6] Ruiz V G, Liu W, Zojer E, Scheffler M and Tkatchenko A 2012 Density-functional theory with screened van der Waals interactions for the modeling of hybrid inorganic-organic systems *Phys. Rev. Lett.* **108** 146103

[7] Mercurio G *et al* 2013 Quantification of finite-temperature effects on adsorption geometries of π-conjugated molecules: azobenzene/Ag(111) *Phys. Rev.* B **88** 035421

[8] Feringa B L and Browne W R (ed) 2011 *Molecular Switches* 2nd edn (Weinheim: Wiley)

[9] Nägele T, Hoche R, Zinth W and Wachtveitl J 1997 Femtosecond photoisomerization of cis-azobenzene *Chem. Phys. Lett.* **272** 489–95

[10] Satzger H, Root C and Braun M 2004 Excited-state dynamics of trans- and cis-azobenzene after uv excitation in the $\pi\pi^*$ band *J. Phys. Chem.* A **108** 6265–71

[11] Comstock M J *et al* 2007 Reversible photomechanical switching of individual engineered molecules at a metallic surface *Phys. Rev. Lett.* **99** 038301

[12] Henningsen N, Franke K J, Torrente I F, Schulze G, Priewisch B, Rück-Braun K, Dokić J, Klamroth T, Saalfrank P and Pascual J I 2007 Inducing the rotation of a single phenyl ring with tunneling electrons *J. Phys. Chem.* C **111** 14843–8

[13] Alemani M, Selvanathan S, Ample F, Peters M V, Rieder K-H, Moresco F, Joachim C, Hecht S and Grill L 2008 Adsorption and switching properties of azobenzene derivatives on different noble metal surfaces: Au (111), Cu(111), and Au(100) *J. Phys. Chem.* C **112** 10509–14

[14] Óvári L, Schwarz J, Peters M V, Hecht S, Wolf M and Tegeder P 2008 Reversible isomerization of an azobenzene derivative adsorbed on Au(111): analysis using vibrational spectroscopy *Int. J. Mass Spectrom.* **277** 223–8

[15] Bronner C, Schulze G, Franke K J, Pascual J I and Tegeder P 2011 Switching ability of nitro-spiropyran on Au(111): electronic structure changes as a sensitive probe during a ring-opening reaction *J. Phys.: Condens Matter* **23** 484005

[16] Bronner C, Schulze M, Hagen S and Tegeder P 2012 The influence of the electronic structure of adsorbate-substrate complexes on photoisomerization ability *New J. Phys.* **14** 043023

[17] Hagen S, Leyssner F, Nandi D, Wolf M and Tegeder P 2007 Reversible switching of tetra-*tert*-butyl-azobenzene on a Au(111) surface induced by light and thermal activation *Chem. Phys. Lett.* **444** 85–90

[18] Schulze G, Franke K J and Pascual J I 2012 Induction of a photostationary ring-opening-ring-closing state of spiropyran monolayers on the semimetallic Bi(110) surface. *Phys. Rev. Lett.* **109** 026102

[19] Pechenezhskiy I V, Cho J, Nguyen G D, Berbil-Bautista L, Giles B L, Poulsen D A, Fréchet J M J and Crommie M F 2012 Self-assembly and photomechanical switching of an azobenzene derivative on GaAs (110): scanning tunneling microscopy study *J. Phys. Chem.* C **116** 1052–5

[20] Bazarnik M, Henzl J, Czajka R and Morgenstern K 2011 Light driven reactions of single physisorbed azobenzenes *Chem. Commun.* **47** 7764–6

[21] Karcher M, Rüdt C, Elsäßer C and Fumagalli P 2007 Switching of nonfunctionalized spiropyran thin films on single crystalline MgO(100) *J. Appl. Phys.* **102** 084904

[22] Óvári L, Luo Y, Leyssner F, Haag R, Wolf M and Tegeder P 2010 Adsorption and switching properties of a N-benzylideneaniline based molecular switch on a Au(111) surface *J. Chem. Phys.* **133** 044707
[23] Frisch J, Herder M, Herrmann P, Heimel G, Hecht S and Koch N 2013 Photoinduced reversible changes in the electronic structure of photochromic diarylethene films *Appl. Phys.* A **113** 1–4
[24] Koshima H, Ojima N and Uchimoto H 2009 Mechanical motion of azobenzene crystals upon photoirradiation *J. Am. Chem. Soc.* **131** 6890–1
[25] Kobatake S, Takami S, Muto H, Ishikawa T and Irie M 2007 Rapid and reversible shape changes of molecular crystals on photoirradiation *Nature* **446** 778–81
[26] Füchsel G, Klamroth T, Dokić J and Saalfrank P 2006 On the electronic structure of neutral and ionic azobenzenes and their possible role as surface mounted molecular switches *J. Phys. Chem.* B **110** 16337–45
[27] Henningsen N, Rurali R, Franke K J, Fernández-Torrente I and Pascual J I 2008 Trans to cis isomerization of an azobenzene derivative on a Cu(100) surface *Appl. Phys.* A **93** 241–6
[28] Henningsen N, Rurali R, Limbach C, Drost R, Pascual J I and Franke K J 2011 Site-dependent coordination bonding in self-assembled metal-organic networks *J. Phys. Chem. Lett.* **2** 55–61
[29] Bronner C, Priewisch B, Rück-Braun K and Tegeder P 2013 Photoisomerization of an azobenzene on the Bi(111) surface *J. Phys. Chem.* C **117** 27031–8
[30] Petek H and Ogawa S 1997 Femtosecond time-resolved two-photon photoemission studies of electron dynamics in metals *Prog. Surf. Sci.* **56** 239–310
[31] Weinelt M 2002 Time-resolved two-photon photoemission from metal surfaces *J. Phys.: Condens. Matter* **14** R1099
[32] Zhu X-Y 2004 Electronic structure and electron dynamics at molecule-metal interfaces: implications for molecule-based electronics *Surf. Sci. Rep.* **56** 1–83
[33] Tegeder P 2012 Optically and thermally induced molecular switching processes at metal surfaces *J. Phys.: Condens. Matter* **24** 394001
[34] Varene E, Bogner L, Meyer S, Pennec Y and Tegeder P 2012 Coverage-dependent adsorption geometry of octithiophene on Au(111) *Phys. Chem. Chem. Phys.* **14** 691–6
[35] Palmberg P W 1972 *Handbook of Auger Electron Spectroscopy* (Edina, MN: Physics Electronics Industries)
[36] Lüth H 1995 *Surfaces and Interfaces of Solid Materials* 3rd edn (Berlin: Springer)
[37] Wegkamp D, Meyer M, Richter C, Wolf M and Stähler J 2013 Photoinduced work function modifications and their effect on photoelectron spectroscopy *Appl. Phys. Lett.* **103** 151603
[38] Zhou X-L, Zhu X-Y and White J M 1991 Photochemistry at adsorbate/metal interfaces *Surf. Sci. Rep.* **13** 73–220
[39] Hasselbrink E 1994 Mechanisms in photochemistry on metal surfaces *Appl. Surf. Sci.* **79-80** 34–40
[40] Hagen S, Kate P, Peters M V, Hecht S, Wolf M and Tegeder P 2008 Kinetic analysis of the photochemically and thermally induced isomerization of an azobenzene derivative on Au(111) probed by two-photon photoemission *Appl. Phys.* A **93** 253–60
[41] Piantek M *et al* 2009 Reversing the thermal stability of a molecular switch on a gold surface: ring-opening reaction of nitrospiropyran *J. Am. Chem. Soc.* **131** 12729–35
[42] Mielke J, Leyssner F, Koch M, Meyer S, Luo Y, Selvanathan S, Haag R, Tegeder P and Grill L 2011 Imine derivatives on Au(111): evidence for inverted thermal isomerization *ACS Nano* **5** 2090–7
[43] Weigelt S, Busse C, Petersen L, Rauls E, Hammer B, Gothelf K V, Besenbacher F and Linderoth T R 2006 Chiral switching by spontaneous conformational change in adsorbed organic molecules *Nat. Mater.* **5** 112–7